BNL-104782-2014-TECH

AGS/AD/Tech Note No. 366;BNL-104782-2014-IR

Wiggler Snakes for RHIC

M. Conte

September 1992

Collider Accelerator Department

Brookhaven National Laboratory

U.S. Department of Energy

USDOE Office of Science (SC)

DISCLAIMER

Accelerator Division
Alternating Gradient Synchrotron Department
BROOKHAVEN NATIONAL LABORATORY
Upton, New York 11973

Accelerator Division
Technical Note

AGS/AD/Tech. Note No. 366

Wiggler Snakes for RHIC

Mario Conte* and Alfredo Luccio

September 21, 1992

Introduction

Snakes inserted in RHIC to rotate the spin of the proton from vertical to radial and conversely can be built with two series of magnets, each series with magnetic fields directed along the vertical and radial axes respectively. The two series are longitudinally shifted respect to each other, as schematically shown in figure 1. The simplest configuration has three horizontal dipoles and three vertical. In each configuration the magnetic field integral must be zero, so that a proton entering the structure on axis would also emerge on axis.

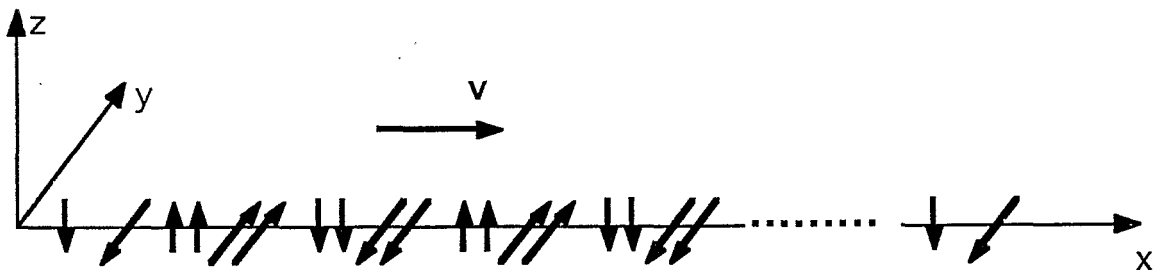

Fig.1 Spin rotator with transverse magnets.

Configurations with more than six dipoles (wiggler snakes) have pros and cons.

Advantages are:

smaller overall magnet volumes. This is particularly important in RHIC, where adjacent beamlines are very close together (40-50cm) near the interaction regions;

smaller beam displacement, expecially important at lower proton energies (injection);

lower electric power;

possibility of using permanent magnets;

---

* Permanent Address: Dip. di Fisica, Università di Genova, Italy

use of proton undulator radiation (synchrotron), in its harmonics, for non destructive beam diagnostics.

Disadvantages are:

greater snake length.

We have studied the behaviour of a series of wiggler snakes, both with conventional and superconducting magnets. The results are described in the following.

Equations

The proton beam propagates along the x-axis (figure 1). z is the vertical axis and y the transverse axis.

The spin rotation was calculated by numerical integration of the vector equation for the unitary spin vector $\hat{s}$ in a given transverse magnetic field

(1) $$\frac{d\hat{s}}{dt} = \Omega \times \hat{s} = -\frac{e}{m\gamma}(1+G\gamma)\boldsymbol{B}_{\perp} \times \hat{s}$$

with

(2) $$G = 1.7928 \quad ; \quad \frac{e}{m} = 9.58\,10^{7}\,\mathrm{sec}^{-1}\,\mathrm{T}^{-1}$$

and γ the relativistic energy of the protons.

In scalar form

(3) $$\begin{cases} \dot{s}_x = \Omega_y s_z - \Omega_z s_y \\ \dot{s}_y = \Omega_z s_x \qquad ; \quad s_x^2 + s_y^2 + s_z^2 = 1 \\ \dot{s}_z = -\Omega_y s_x \qquad\quad s_x\dot{s}_x + s_y\dot{s}_y + s_z\dot{s}_z = 0 \end{cases}$$

The scalar equations for the trajectory are

(4) $$y,z(x) = \int \frac{I_{z,y}(x)}{\sqrt{1-I_{z,y}^2(x)}}\,dx$$

with the first field integral

(5) $$I_{z,y}(x) = \frac{e}{\beta\gamma mc}\int B_{z,y}(x)\,dx$$

A proton on axis at the entrance will emerge on axis if this integral is zero for the whole snake.

The integration of the six equations (3) + (4), using x as the independent variable, was performed by a Runge-Kutta plus Predictor Corrector routine.

The synchrotron radiation generated by the high energy protons in the wiggler snakes will exhibit a line spectrum with fundamental wavelength given by

$$\lambda_1 = \lambda_0 \frac{1+\frac{k^2}{2}}{2\gamma^2} \quad ; \quad k = \frac{e}{2\pi mc}\lambda_0 B = 0.05086\lambda_0[\mathrm{m}]B[\mathrm{T}] \tag{6}$$

where k is a quantity defining the maximum bending angle of the trajectory in units of $1/\gamma$. When $k<1$ the radiation exhibits the characteristics of undulator radiation.

λ_o is the period of the wiggler, i.e. the length of a full field spatial oscillation alon the x axis. For a three pole snake, the extension of the central field peak is just $\lambda_o/2$.

Results

Results of the calculations for wiggler/snakes capable of rotating the polarization between y and z are shown in Table 1. The values are calculated for $\gamma = 200$, however, they are in very good approximation valid for a very wide range of proton energies, as Equation (1) readily shows.

Entries in Table 1 are for normal conducting and superconducting magnets. Normal magnets may be substituted by permanent magnets. The total length L of a snake including the two end poles of half strength, the total relative snake volume V and the relative magnetic field energy W are estimated as follows

$$L = (n+1)\frac{\lambda_0}{2} \quad ; \quad V = L\lambda_0^2 \quad ; \quad W = (n+1)\lambda_0^2 B^2 \tag{7}$$

The expression for the volume relies on the observation that the transverse dimensions of each component dipole are of the order of the period, and for the energy stored in the field (then the required electric power) on the observation that the energy is proportional to the volume of the magnetc gap. Thus, we disregard the energy stored in the steel. which is not probably accurate for the superconducting magnets.

Column 4 is the number of full field dipoles of half period length. This number must be odd. Column 7 is the fundamental wavelength of the radiation: it always lies in the infrared, however its odd harmonics, say the 5th, 7th and 9th, are in the near infrared or in the visbile, then easily detectable. The last column is a reference to the case # and to the figures.

In order to achieve the appropriate field integral to obtain the desired spin rotation, the product $\lambda_o B$ is only slowly growing. Accordingly, the length of a multipole snake grovs not too fast with n so that a 15-pole is about twice as long than a 1-pole. Indeed the volume decreases, and with it the magnet cost should also do, in spite of the greater complication of fabrication. The energy stored in the magnetic field also decreases for normal conducting snakes.

Table 1

B [T]	λ_o [m]	L [m]	n	V	W	λ_1 [μm]	#
			Normal Conducting				
1.728	6.0	6.0	1	216	215	85.40	6-6
	3.6	7.2	3	93	155	47.25	7-5
	2.8	8.4	5	66	141	36.06	7-8
	2.4	9.6	7	55	138	30.67	7-11
	2.1	10.2	9	45	132	26.70	7-13
	1.9	11.4	11	41	129	24.08	7-15
	1.75	12.3	13	38	128	22.13	7-17
	1.63	13.0	15	35	127	20.58	7-20
1.85	1.52	12.2		28	127	19.19	7-21
			Superconducting				
2.6	1.08	8.64		10	126	13.64	8-1
3.2	0.88	7.04		6	126	11.11	8-7
4.0	0.70	5.60		3	125	8.84	8-8
5.0	0.56	4.48		2	125	7.07	8-9
6.0	0.47	3.76		1	127	5.94	8-10

The figures 1 through 15 show the results of the integration of equations (2) and (4) for the spin components and for the proton orbits. In the representation of the spin behaviour the conventions are the following

thin lines are the field components

B_y ———— B_z ·····

thick lines are the spin components

S_x ———— S_y ····· S_z - - - - - -

and the trajectory

z (vertical) ———— y (radial) ·····

Figures 2-6 show the spin transition and proton trajectories for a 1-pole (plus end poles) normal conducting snake. Figures 7-11 show the spin transition for 3, 5, 11 and 15 poles, normall conducting, respectively. Figure 12 shows the trajectory for 15 poles.

Figures 13-20 show spin precession and trajectories for superconducting 15-pole snakes.

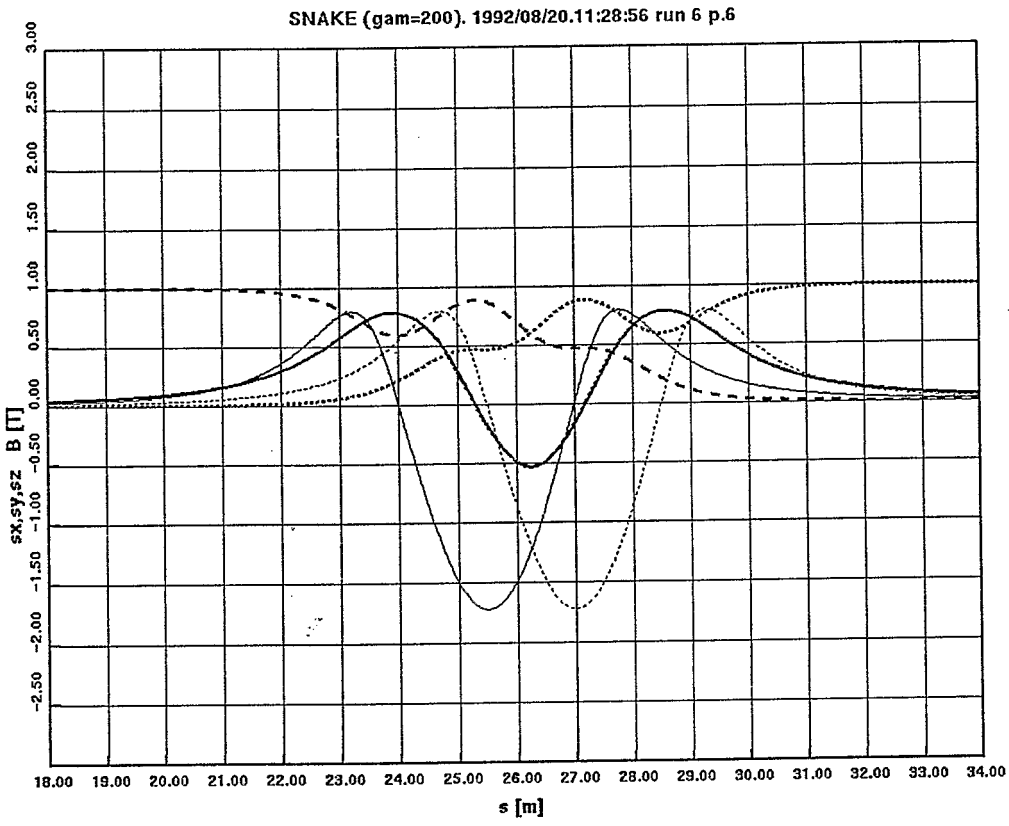

Fig.2. Transition for a 1-pole snake. Spin from vertical to radial. S_x is unchanged

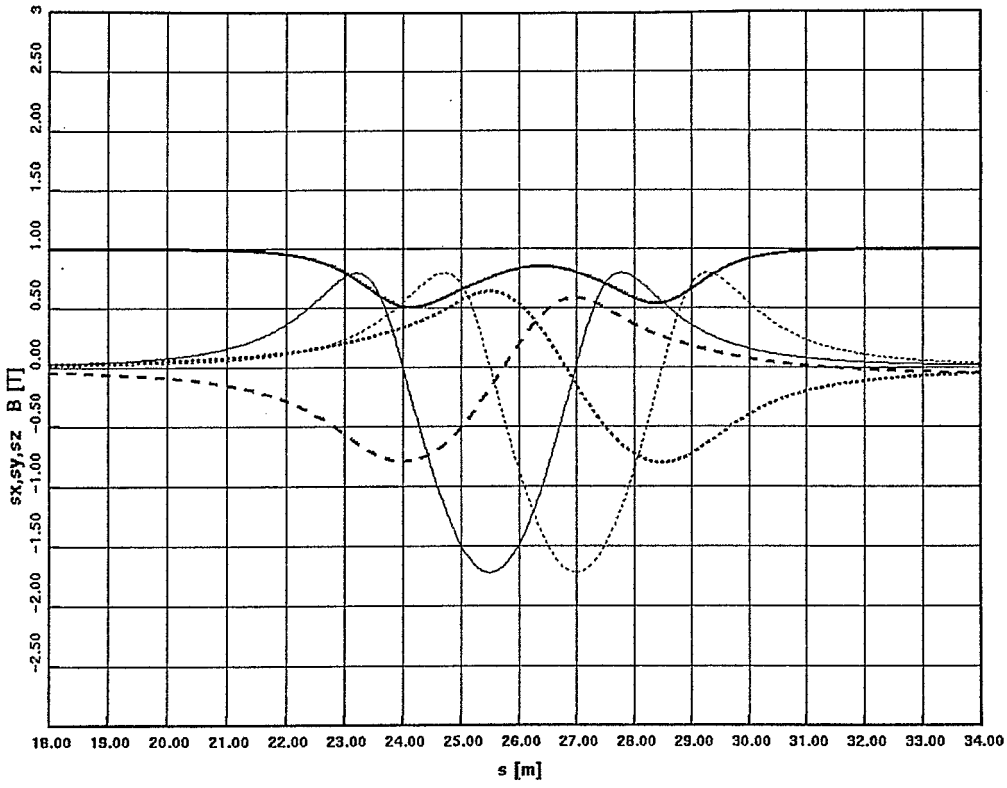

Fig.3. Transition for a 1-pole snake. Spin (longitudinal) is unchanged

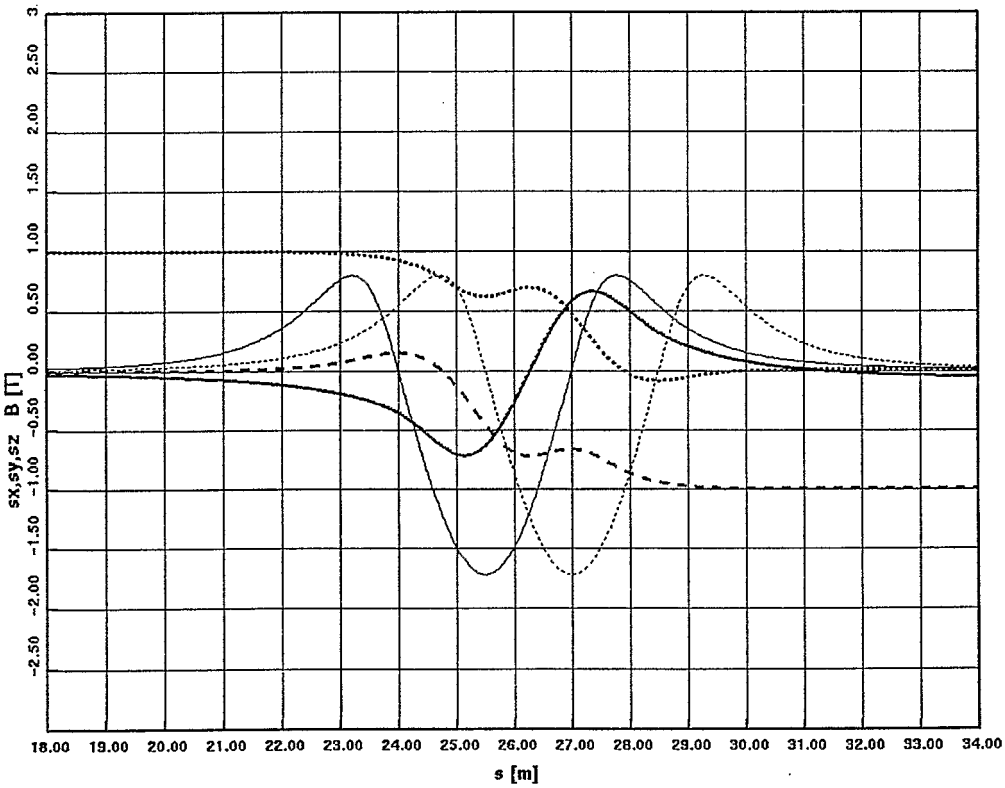

Fig.4. Transition for a 1-pole snake. Spin from vertical to radial. S_x is unchanged

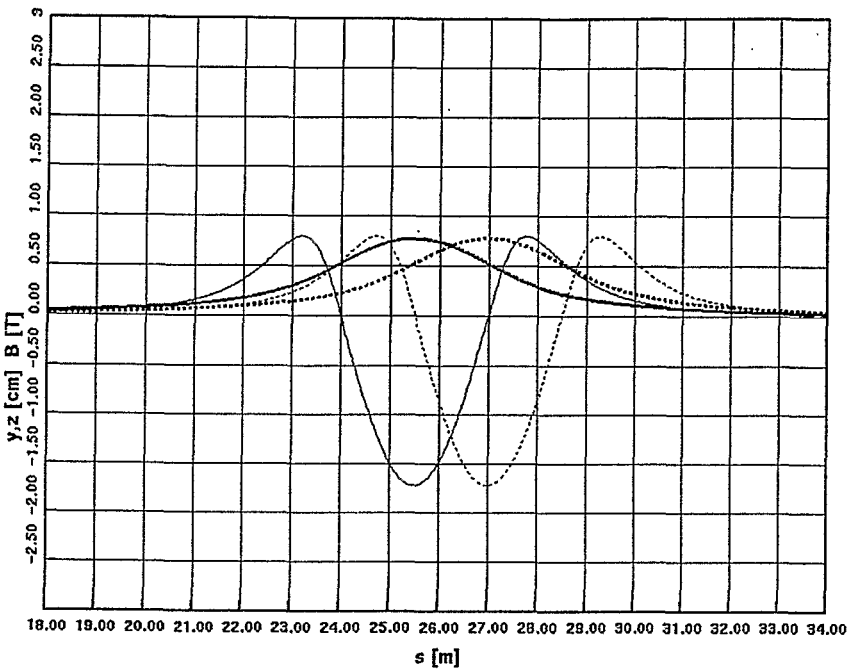

Fig 5. Trajectory in a 1-pole snake. $\gamma = 200$.

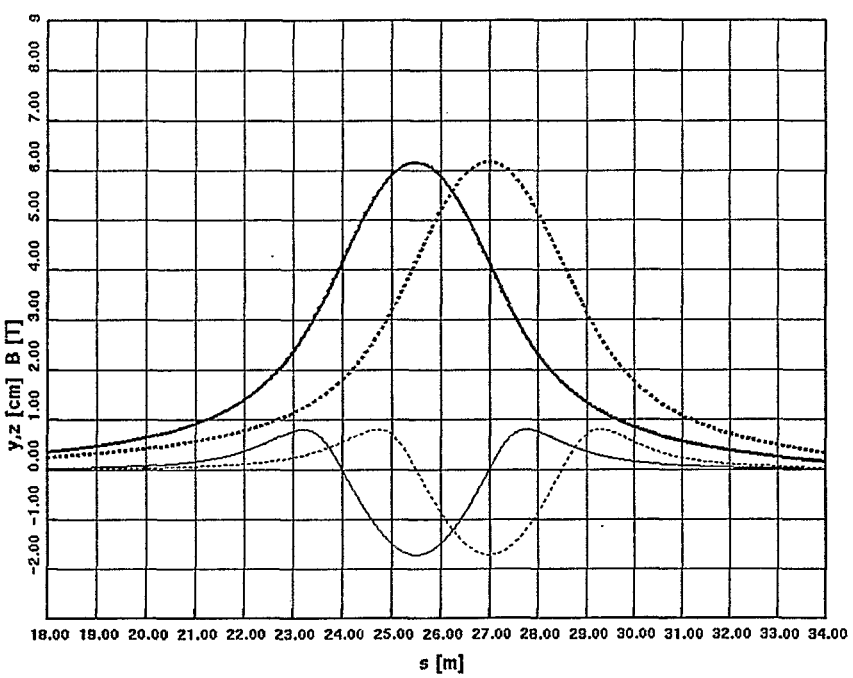

Fig.6. Trajectory in a 1-pole snake. $\gamma = 25$.

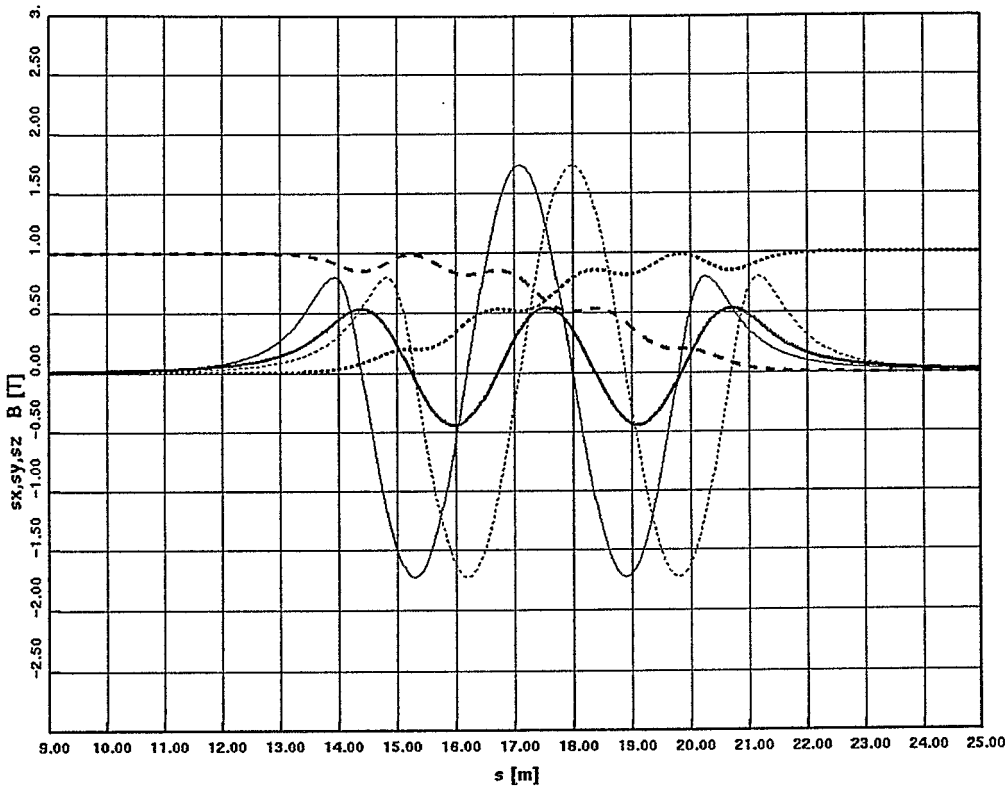

Fig.7. Transition for a 3-pole snake. Spin from vertical to radial. S_x is unchanged

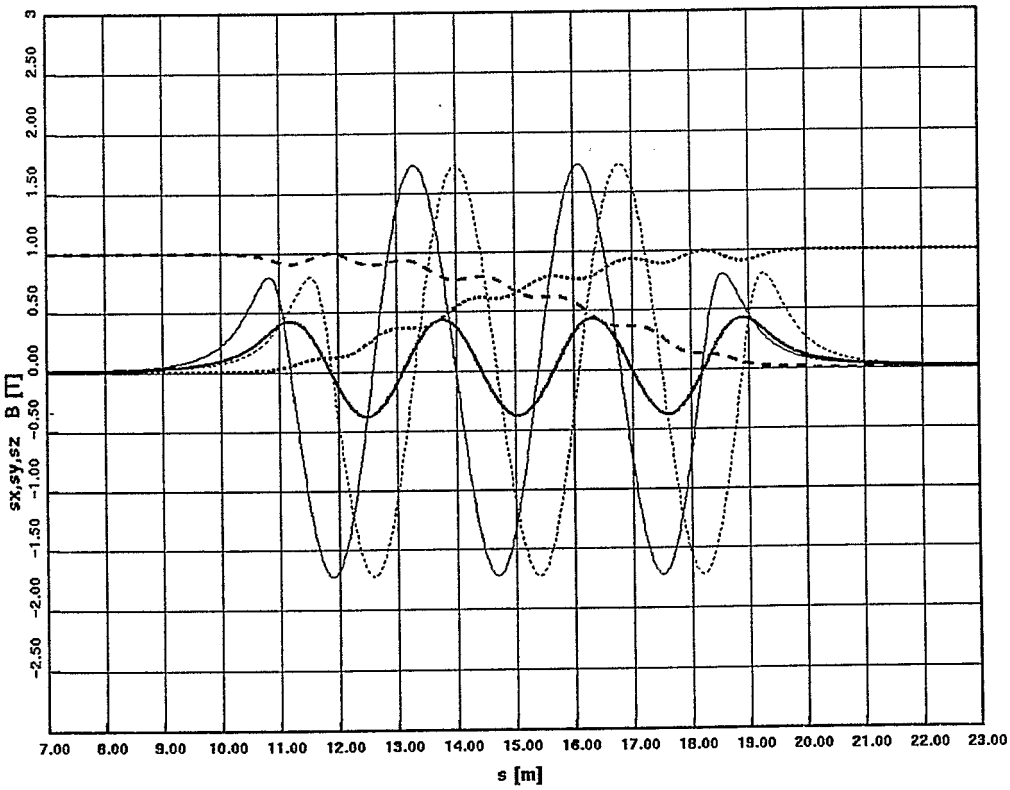

Fig.8. Transition for a 5-pole snake. Spin from vertical to radial. S_x is unchanged

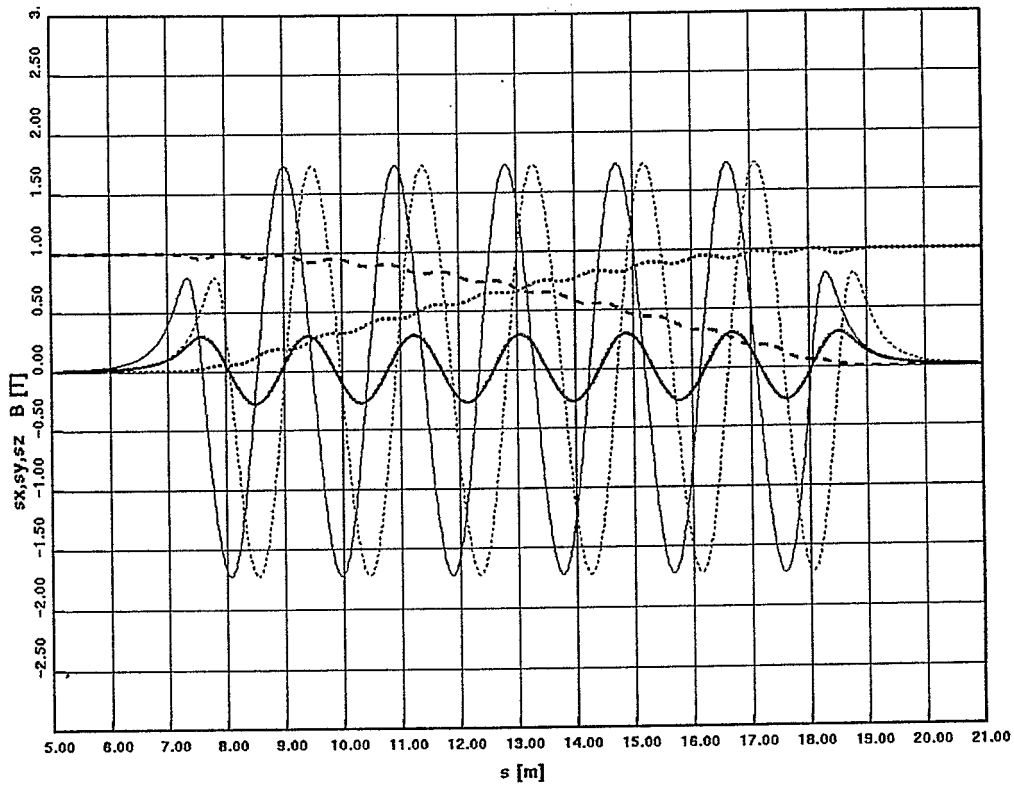

Fig.9. Transition for a 11-pole snake. Spin from vertical to radial. S_x is unchanged

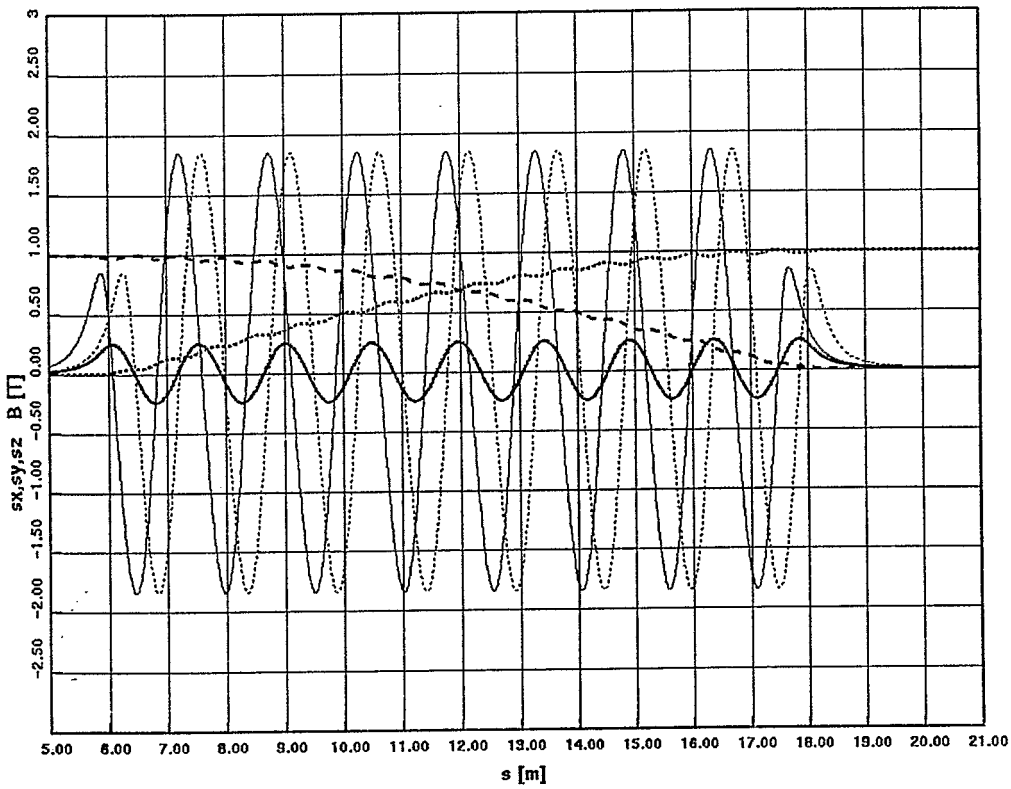

Fig.10. Transition for a 15-pole snake. Spin from vertical to radial. S_x is unchanged

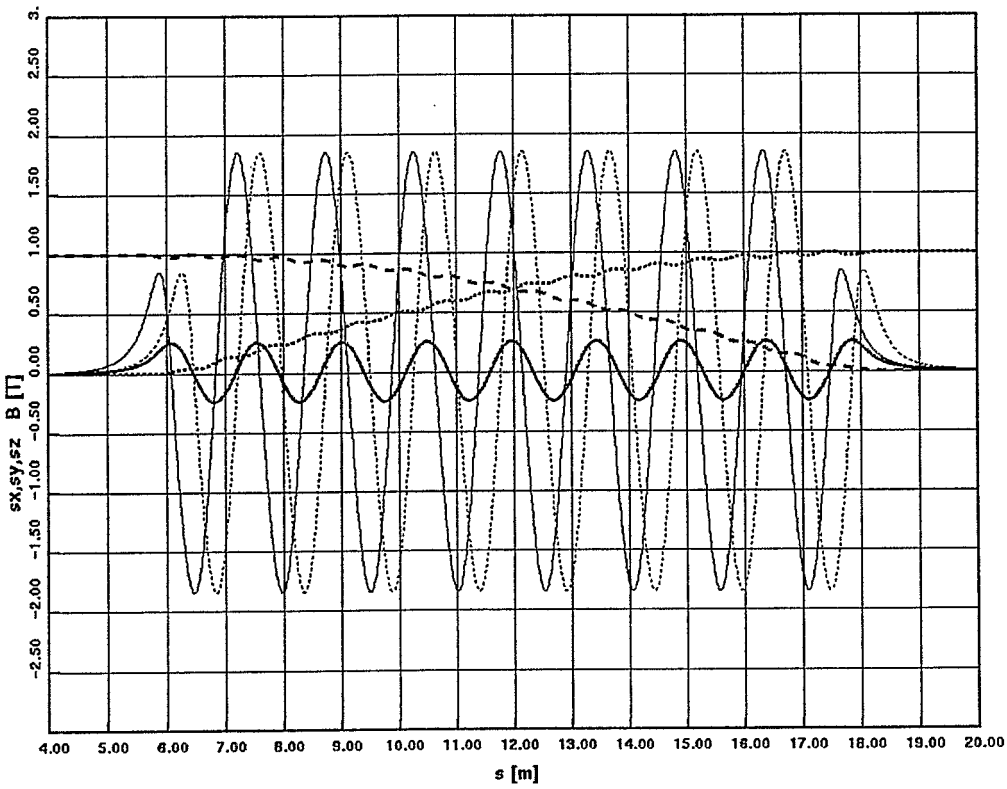

Fig.11. Transition for a 15-pole snake. Spin from vertical to radial. S_x is unchanged

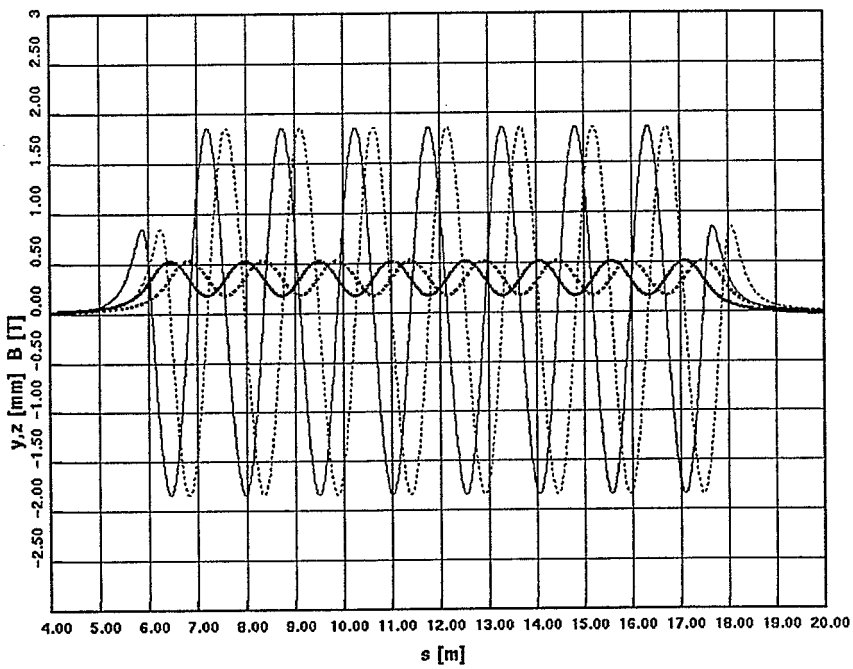

Fig.12. Trajectory in the 15-pole snake of Fig.11. $\gamma = 200$.

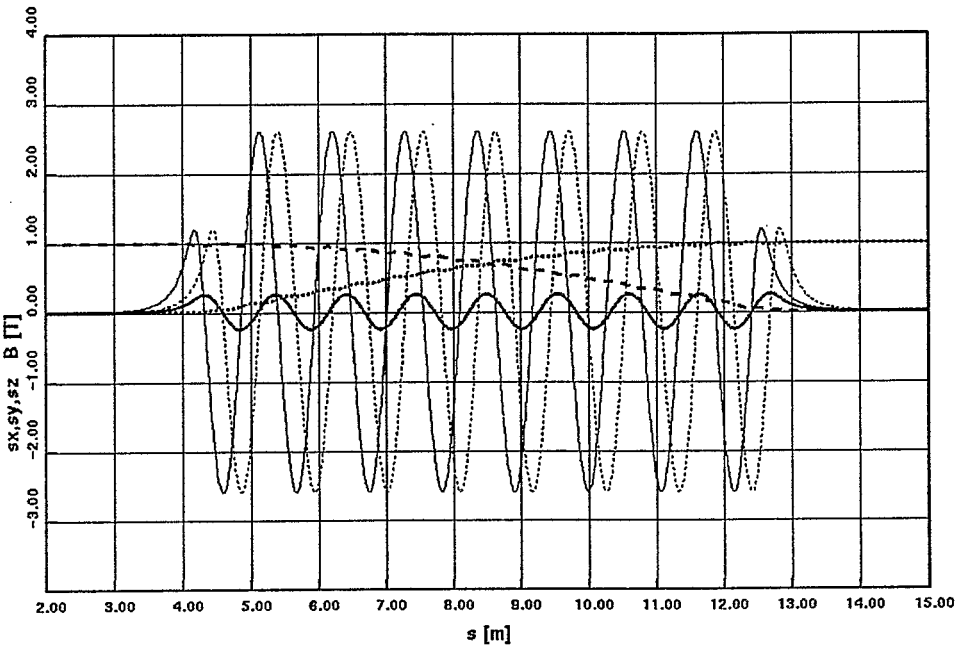

Fig.13. Transition for a 15-pole SC snake. Spin from vertical to radial. S_x is unchanged

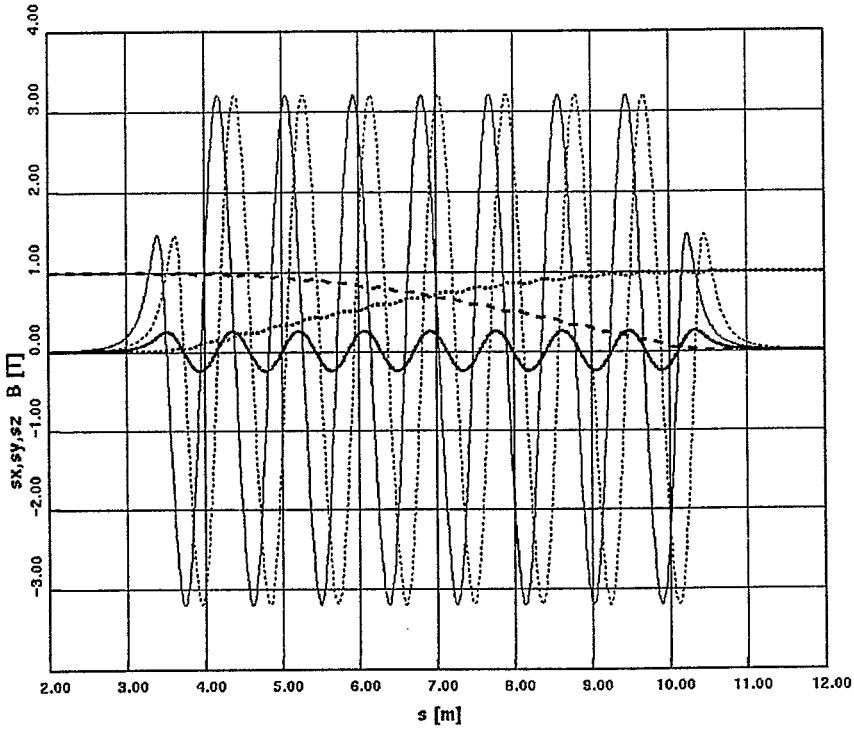

Fig.14. Transition for a 15-pole SC snake. Spin from vertical to radial. S_x is unchanged

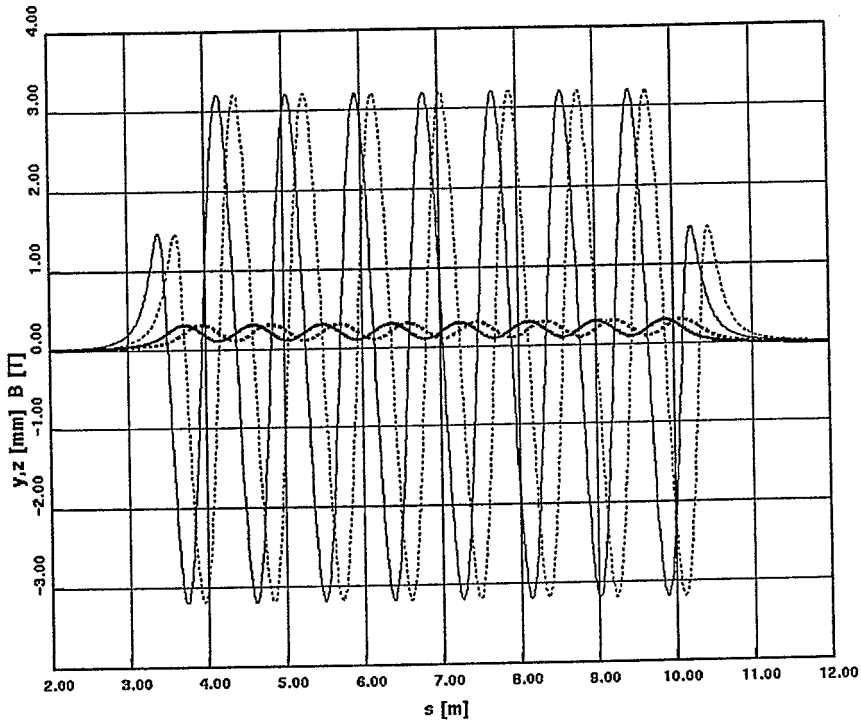

Fig.15. Trajectory in the 15-pole SC snake of Fig.14. $\gamma = 200$.

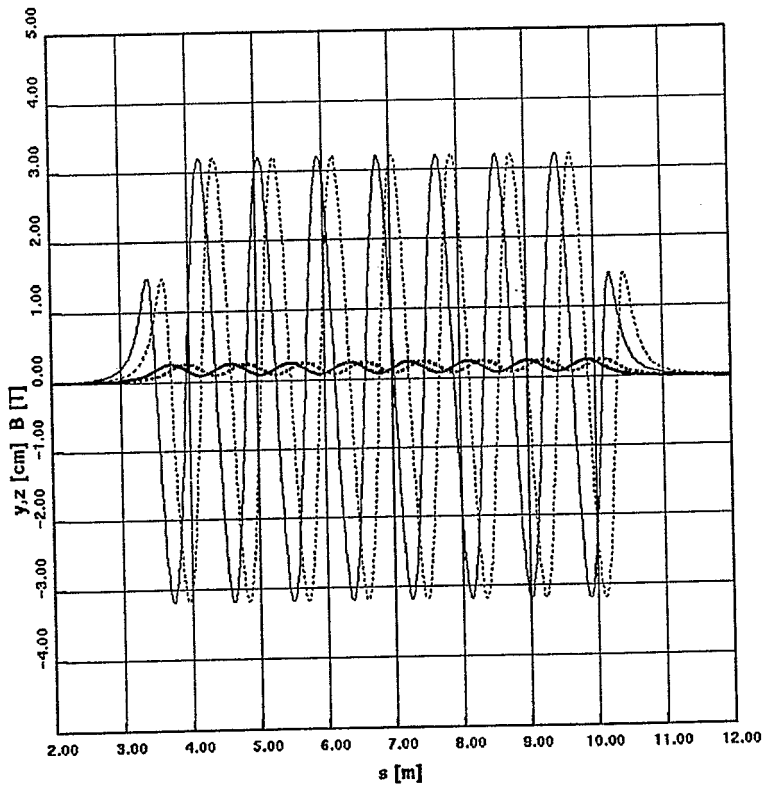

Fig.16. Trajectory in the 15-pole SC snake of Fig.14. $\gamma = 25$.

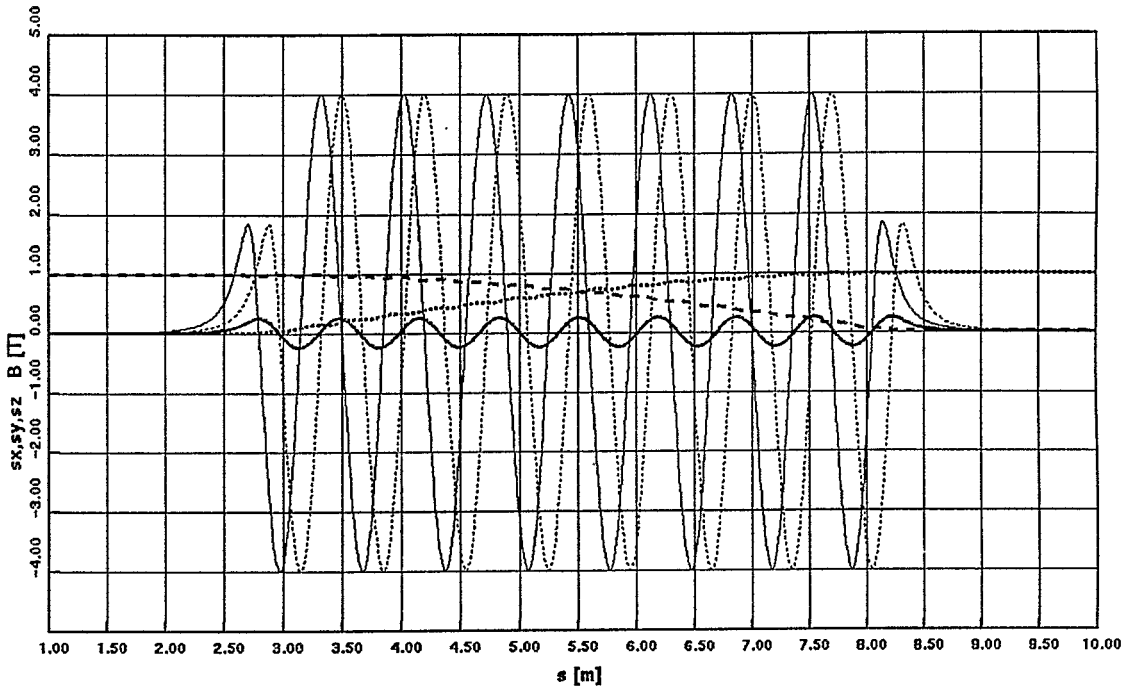

Fig.17. Transition for a 15-pole SC snake. Spin from vertical to radial. S_x is unchanged

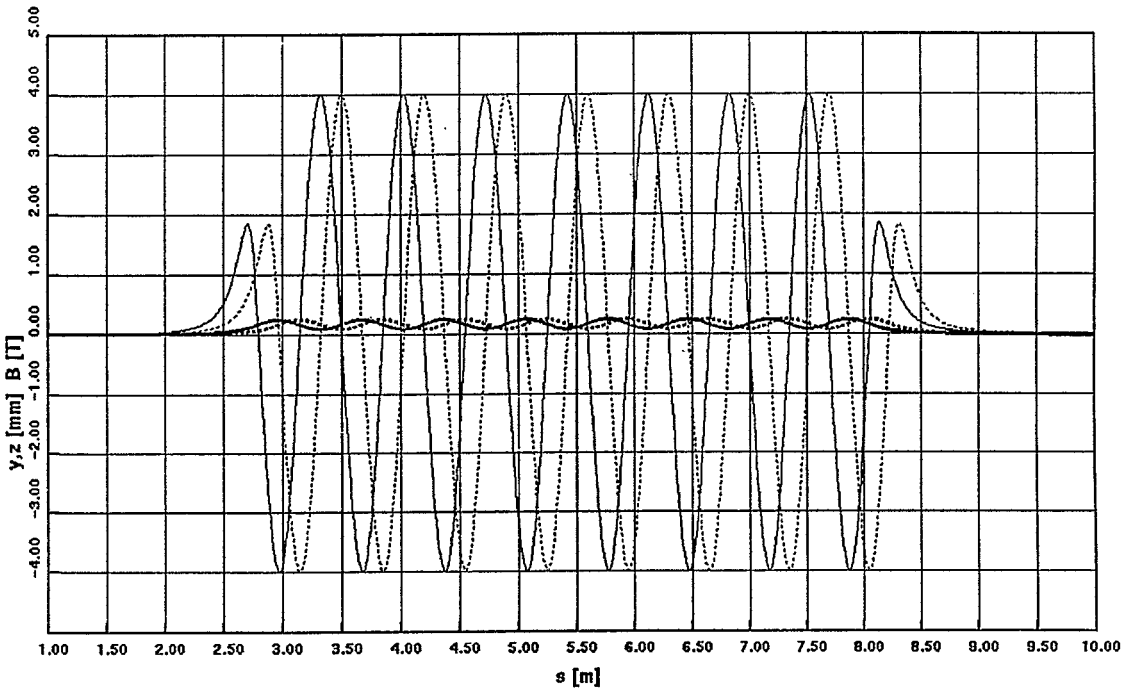

Fig.18. Trajectory in the 15-pole SC snake of Fig.17. $\gamma = 200$.

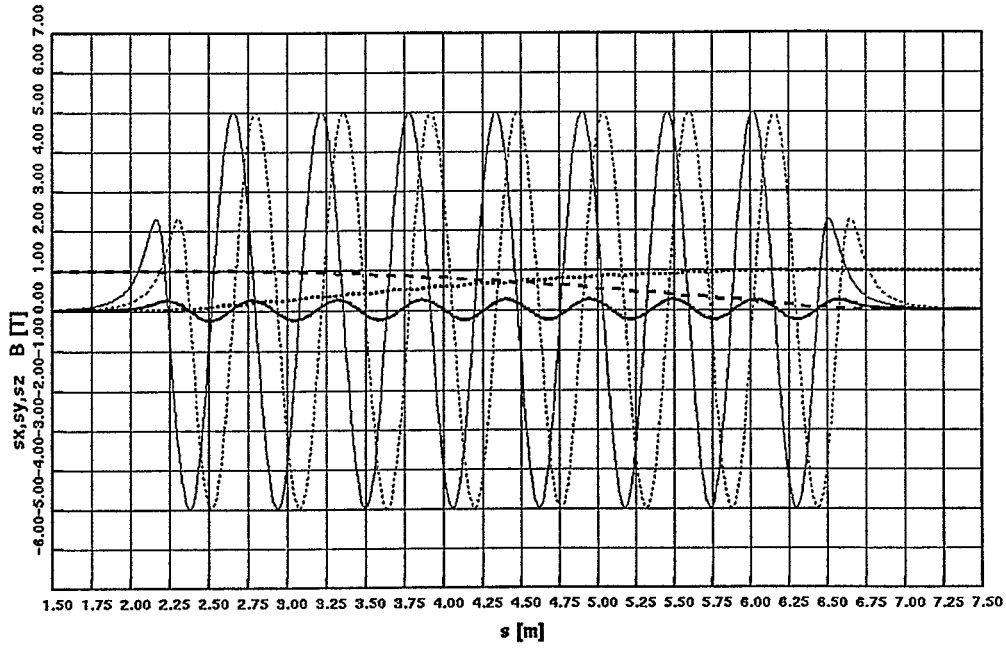

Fig.19. Transition for a 15-pole SC snake. Spin from vertical to radial. S_x is unchanged

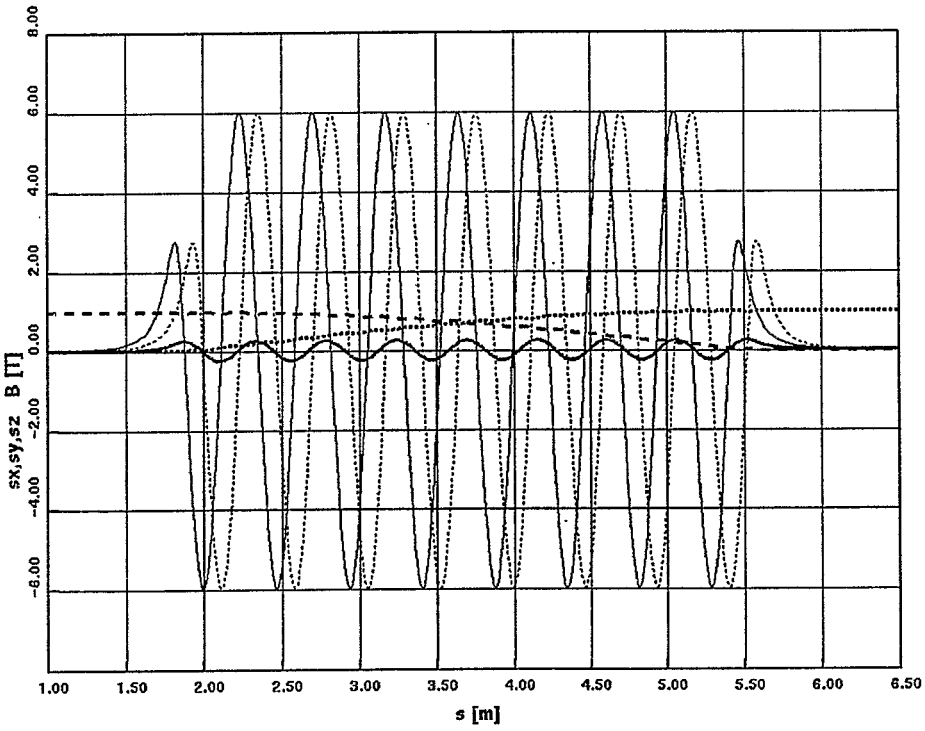

Fig.20. Transition for a 15-pole SC snake. Spin from vertical to radial. S_x is unchanged

Snake structure

A strong reason to propose transversely small snakes for RHIC is the proximity of adiacent beam lines. A possible structure is the double barrel shown in Figures 21-24.

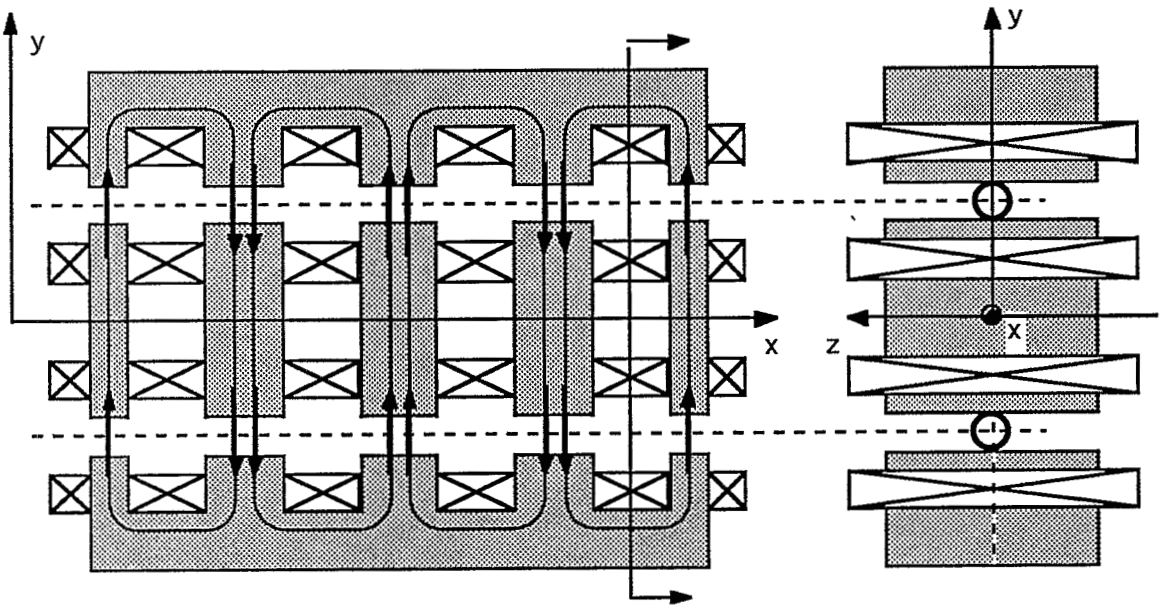

Fig.21. Double barrel, n=3, longitudinal section. Radial field parallel in the two beamlines

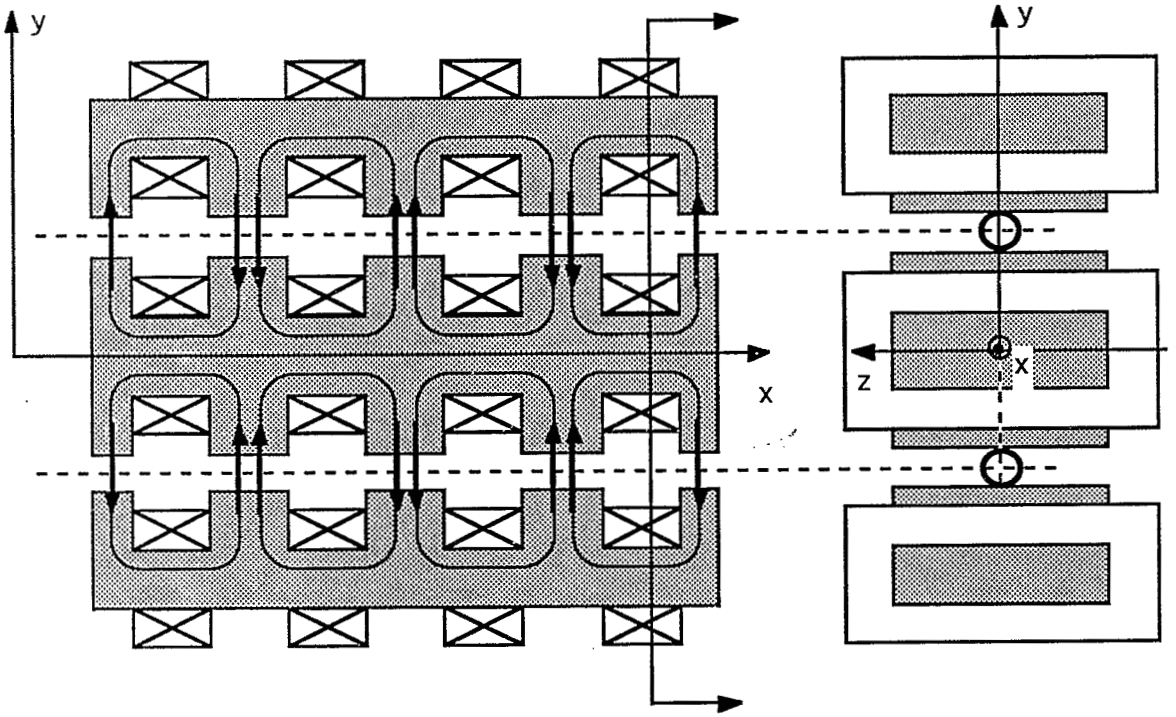

Fig.22. Double barrel, n=3. Longitudinal cut. Vertical field antiparallel in the beam lines.

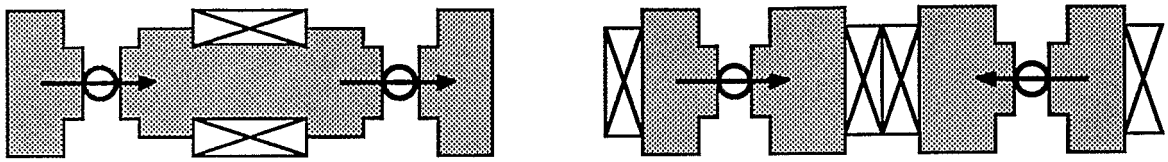

(a) (b)

Fig.23. Double barrel. Transversal cut. Horizontal field, a) parallel, b) antiparallel.

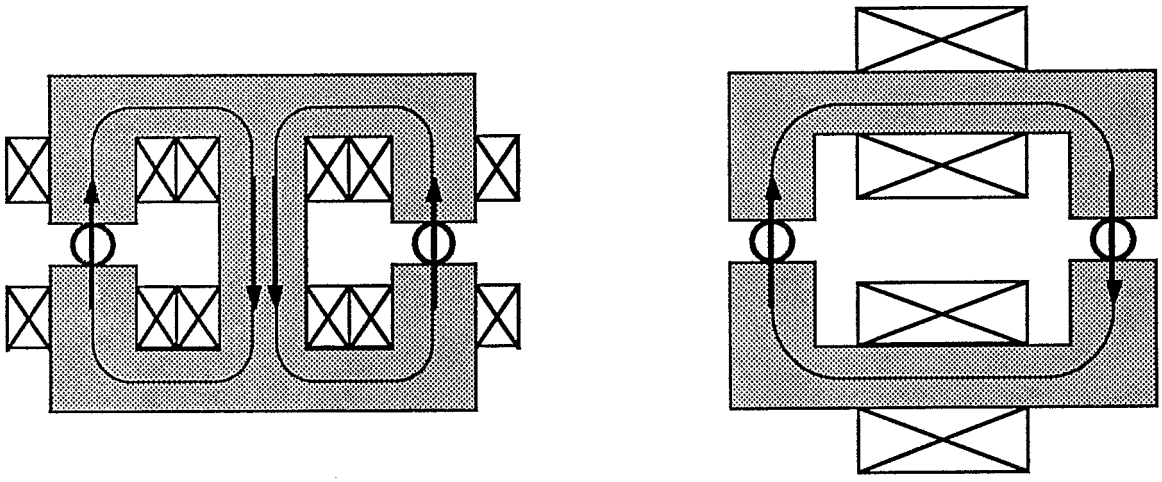

(a) (b)

Fig.24. Double barrel. Transversal cut. Vertical field a) parallel, b) antiparallel.